J|A|C|S COMMUNICATIONS

Published on Web 10/14/2010

De Novo Design and Molecular Assembly of a Transmembrane Diporphyrin-Binding Protein Complex

Ivan V. Korendovych,[†] Alessandro Senes,[†,⊥] Yong Ho Kim,[†] James D. Lear,[†] H. Christopher Fry,[||] Michael J. Therien,[‡] J. Kent Blasie,[||] F. Ann Walker,[§] and William F. DeGrado*[,†,||]

Department of Biochemistry and Biophysics, University of Pennsylvania, Philadelphia, Pennsylvania 19104, Department of Chemistry, Duke University, Durham, North Carolina 27708, Department of Chemistry and Biochemistry, University of Arizona, Tucson, Arizona 85721, and Department of Chemistry, University of Pennsylvania, Philadelphia, Pennsylvania 19104

Received August 18, 2010; E-mail: wdegrado@mail.med.upenn.edu

Abstract: The de novo design of membrane proteins remains difficult despite recent advances in understanding the factors that drive membrane protein folding and association. We have designed a membrane protein PRIME (PoRphyrins In MEmbrane) that positions two non-natural iron diphenylporphyrins (Fe^{III}DPP's) sufficiently close to provide a multicentered pathway for transmembrane electron transfer. Computational methods previously used for the design of multiporphyrin water-soluble helical proteins were extended to this membrane target. Four helices were arranged in a D_2-symmetrical bundle to bind two Fe(II/III) diphenylporphyrins in a bis-His geometry further stabilized by second-shell hydrogen bonds. UV−vis absorbance, CD spectroscopy, analytical ultracentrifugation, redox potentiometry, and EPR demonstrate that PRIME binds the cofactor with high affinity and specificity in the expected geometry.

Significant progress has been achieved in the computational design of functional water-soluble proteins.[1−6] However, the de novo design of membrane proteins remains difficult despite recent advances in understanding the factors that drive membrane protein folding and association.[7] Here, we present the de novo design of a membrane protein PRIME (PoRphyrins In MEmbrane) that utilizes a non-natural iron diphenylporphyrin (Fe^{III}DPP) with the ultimate goal of facilitating electron transfer across a bilayer. Transmembrane (TM) electron transfer lies at the heart of photosynthesis and ATP production in a variety of organisms and thus is of great fundamental interest and, potentially, of practical importance.

Considerable progress has been made in the design of water-soluble multiheme proteins[8−11] and amphiphilic maquettes[12−15] that position a single heme in the membrane phase. Also, in an elegant study, Cordova et al.[16] designed a TM peptide that binds a single heme between two helices whose geometry is defined by a GXXXG motif. To be generally useful for transmembrane electron transfer, it is important to also design systems that position multiple redox-active cofactors sufficiently close to provide a multicentered pathway for electrons to rapidly pass across the bilayer.

Here we extend previous computational methods used for the design of water-soluble multiheme proteins to membrane targets. The design of PRIME is based on the backbone of a water-soluble multiporphyrin-binding peptide.[17,18] Its fold appeared to be particularly well suited for a membrane environment, because it has a tight interhelical "Ala-coil" motif, which is favored in both water and membrane-soluble proteins.[19] Four helices were arranged in a D_2-symmetrical bundle to bind two Fe(II/III) diphenylporphyrins in a bis-His geometry. In the design, the His ligands are stabilized by a bifurcated second-shell hydrogen bond with a main chain carbonyl and a Thr (T18) hydroxyl from a neighboring helix (Figure 1).[20]

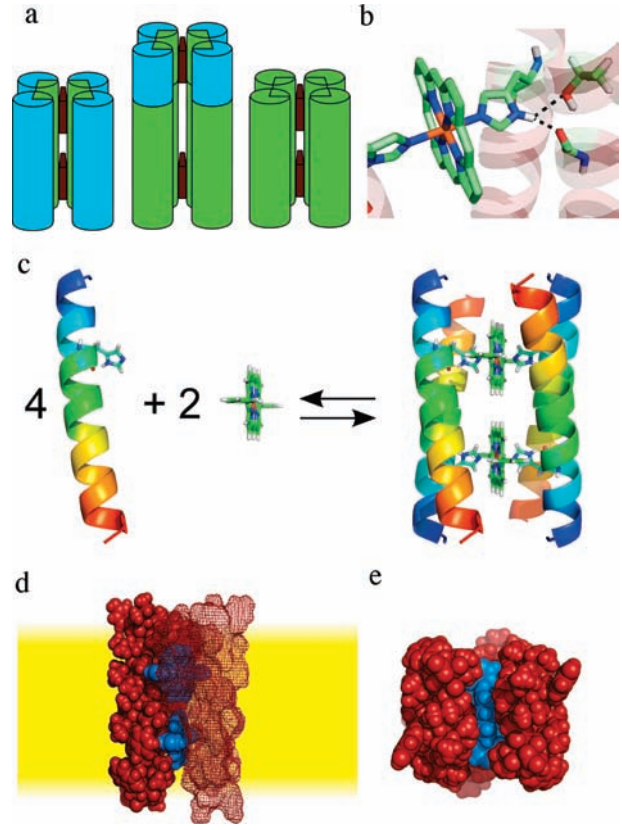

Figure 1. (a) Evolution of the four-helix porphyrin binding bundles: from water-soluble proteins through amphiphilic maquettes to PRIME. Hydrophilic residues are shown in blue, hydrophobic residues are shown in green, and metal cofactor is shown in brown. (b) The design of the iron coordination site in PRIME. (c) General approach to the design of PRIME. The final repacked model of PRIME in a bilayer (yellow) viewed along the directions parallel (d) and normal (e) to the membrane. The sequence of PRIME is Ac-**AIYGILAHSL ASILALLTGF LTIW**-$CONH_2$.

Following the optimization of the coordination sphere of the iron, the backbone was repacked to produce a final sequence. Side chains were selected from an extended, energy-based conformer library (Supporting Information) using Dead End Elimination, followed

[†] Department of Biochemistry and Biophysics, University of Pennsylvania.
[‡] Duke University.
[||] Department of Chemistry, University of Pennsylvania.
[§] University of Arizona.
[⊥] Present address: Department of Biochemistry, University of Wisconsin—Madison.

10.1021/ja107487b

by Monte Carlo/Self Consistent Mean Field. Pairwise energies were calculated with the CHARMM22 force field and Lazaridis implicit membrane solvation (IMM1). Models were ranked by oligomerization energy, i.e. the difference between the energy of the complex and that of the monomeric state (a membrane solvated helical state, with relaxed side chain conformations), and the lowest energy model was chosen for experimental characterization. The two iron(III) diphenylporphyrin molecules in the PRIME model form a path for electron transfer across the membrane. The cofactor in the model is partially accessible near the ends of the bundle to allow water-soluble reagents to access the cofactors (Figure 1).

PRIME is insoluble in water but could be solubilized in detergent micelles and phospholipid bilayers. UV−vis spectroscopy and analytical ultracentrifugation demonstrated that the peptide assembled with the iron(III) diphenylporphyrin cofactor in the expected stoichiometry when solubilized in dodecyl phosphatidylcholine (DPC) micelles. Analytical ultracentrifugation showed that PRIME is predominantly monomeric in DPC micelles in the absence of the cofactor. However in the presence of the cofactor the assembly occurs in a fully cooperative process, and the holoprotein is greater than 90% formed at tetramer/detergent concentrations greater than 1:400 (Figures S1−S5, Supporting Information). The binding of the cofactor (12 μM) was also monitored by the shift in the maximum and intensity of the Soret band upon addition of the peptide at various concentrations. The titration curve (Figure 2) is typical of a tight-binding isotherm with a clean break at a stoichiometry of two peptides per porphyrin as expected for a diporphyrin four-helix bundle. The stoichiometry was additionally confirmed by a Job's plot (Figure S6, Supporting Information). Spectrophotometric titrations also showed that PRIME associated more weakly with the closely related hemin and octaethylporphyrin (Figures 2 and S7, Supporting Information). Additionally, mutation of key residues A15 and G19 to isoleucine, which introduces steric clashes around the porphyrin binding cleft, effectively eliminates the binding of iron(III) diphenylporphyrin (Figure 2). Mutation of the second-shell ligand T18 to alanine also has a detrimental effect on binding (Figure 2).

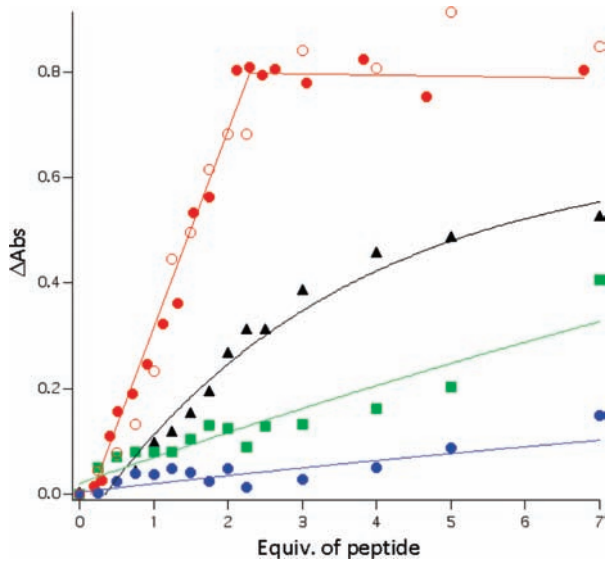

Figure 2. PRIME's specificity. Titration of different cofactors (12 μM) with PRIME peptides. Red circles: Fe^{III}DPP with PRIME (solid circles: slow equilibration method, 2 mM DPC; empty circles: 20 mM DPC); black triangles: hemin with PRIME in DPC (20 mM); green squares: Fe^{III}DPP with PRIME T18A in DPC (20 mM); blue circles: Fe^{III}DPP with PRIME A15I G19I in DPC (20 mM). Cofactor concentration was 12 μM in all cases. Unless explicitly noted, all samples were reconstituted using the fast equilibration method in 10 mM phosphate buffer (pH 7.4) as described in the Supporting Information.

PRIME also binds the cofactor in palmitoyl oleoyl phosphatidylcholine bilayers as evidenced by UV−vis spectra. The position of the Soret band maximum at 410 nm corresponds well to the value observed in micelles (409 nm) (Figure S8, Supporting Information).

CD and EPR spectroscopies showed that the peptide bound the cofactors specifically as intended in the design. CD spectroscopy confirmed the α-helical secondary structure both in the presence and in the absence of the cofactor in DPC micelles (Figure 3). Additionally, binding of the achiral porphyrin to PRIME leads to an induced CD signal in the Soret region of the absorbance spectrum. Negative and positive peak extrema are observed at 415 and 402 nm, respectively, with a crossover point (408 nm) near the maximum in the absorption spectrum (409 nm) (Figure 3). These spectral features are consistent with the exciton coupling expected from the design in which adjacent porphyrins are oriented with a left-handed propeller twist between their porphyrin planes.[21]

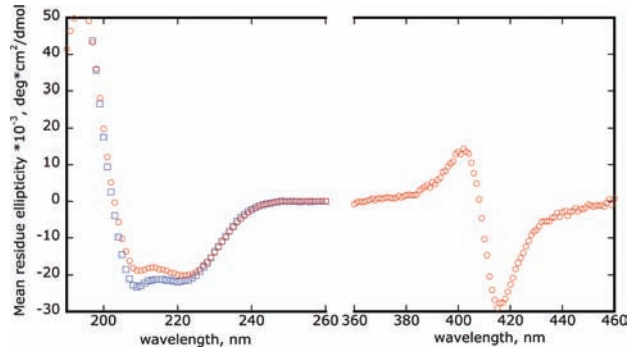

Figure 3. CD spectra of PRIME in the absence (blue) and in the presence (red) of Fe^{III}DPP. Experimental details are given in the Supporting Information. In the case of PRIME-Fe^{III}DPP, MRE values in the 360−460 nm region are normalized to the number of cofactor molecules.

Additional insight into the structure of the designed assembly can be obtained from EPR data. The designed model predicts the angle of 82° between the planes of the His imidazole rings bound to the iron. Such a coordination sphere should result in a "highly anisotropic low spin" (HALS) or Type I iron(III) EPR signal.[22] The observed X-band EPR spectrum agrees well with the prediction: the HALS iron(III) signal ($g = 3.64$) is indeed observed (Figure 4) and is consistent with the spectra of related water-soluble designs 2PA and 4PA.[17,18] The shoulder at $g = 3.37$ is characteristic of a coordination geometry with a somewhat smaller angle between the His planes, yet greater than 60°.[23] Previously studied Fe(III) porphyrin binding maquettes showed multiple peaks between $g =$ 2.0 and 3.0, indicating more relaxed orientations of the His residues.[14]

Reversible chemical reduction of the cofactor is accompanied by the shift in the Soret band maximum to 419 nm and the resolution of the broad Q-band into several components in the 510−560 nm region (Figure S11, Supporting Information), indicative of bis-His ligated low-spin Fe(II) porphyrins.[22] Potentiometric titration of the PRIME-Fe^{III}DPP assembly shows two redox waves (Figure S12, Supporting Information) with apparent $E_{1/2}(Fe^{III}Fe^{III}/Fe^{II}Fe^{III})$ and $E_{1/2}(Fe^{III}Fe^{II}/Fe^{II}Fe^{II})$ of -97 ± 3 mV and -168 ± 3 mV vs NHE, respectively. The 71 mV difference is typical for closely positioned hemes (70−100 mV observed for maquettes with Fe−Fe separation of ∼12 Å),[14] consistent with the design. Interestingly, a similar potential separation (80 mV) is also observed for yeast cytochrome bc_1 hemes b_H and b_L.[24]

In conclusion, we have demonstrated that minimalistic principles combined with computational design can be successfully applied

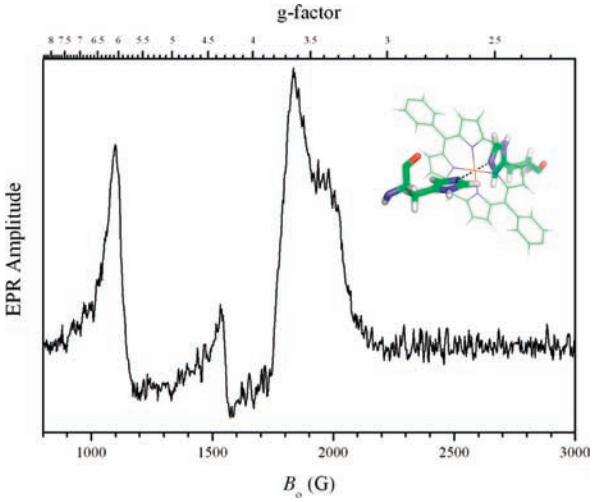

Figure 4. EPR spectrum of Fe^{III}DPP (1.5 mM) bound to PRIME (3.1 mM) in DPC micelles (185 mM) in frozen glass containing 30% glycerol. The peak at $g = 6.0$ represents high-spin iron(III) diphenyl-porphyrin not bound to two histidine residues; the peak at $g = 4.3$ represents a small amount of high-spin nonheme Fe(III).

to create metalloproteins that assemble into well-defined structures exclusively in a membrane environment. In the absence of the hydrophobic driving force we were able to design a membrane peptide PRIME that binds an unnatural cofactor tightly and selectively assembling into a tetrameric bundle. This represents an advance in our understanding of the factors that drive membrane metalloprotein assembly, as well as a major step toward the design of artificial electro- and photosystems.

Acknowledgment. We are grateful to Dr. Andrei V. Astashkin for running the EPR spectra and for estimating the molar ratio of high-spin to low-spin Fe(III) present. We thank Prof. Jeffery G. Saven for helpful discussions. This work was supported by the MRSEC program of the NSF and the NIH, Grant GM54616.

Supporting Information Available: Details of the computational design and experimental characterization of PRIME. This material is available free of charge via the Internet at http://pubs.acs.org.

References

(1) Lu, Y.; Yeung, N.; Sieracki, N.; Marshall, N. M. *Nature* **2009**, *460*, 855–862.
(2) Nanda, V. *Nat. Chem. Biol.* **2008**, *4*, 273–275.
(3) Ghosh, D.; Pecoraro, V. L. *Curr. Opin. Chem. Biol.* **2005**, *9*, 97–103.
(4) Faiella, M.; Andreozzi, C.; de Rosales, R. T. M.; Pavone, V.; Maglio, O.; Nastri, F.; DeGrado, W. F.; Lombardi, A. *Nat. Chem. Biol.* **2009**, *5*, 882–884.
(5) Röthlisberger, D.; Khersonsky, O.; Wollacott, A. M.; Jiang, L.; DeChancie, J.; Betker, J.; Gallaher, J. L.; Althoff, E. A.; Zanghellini, A.; Dym, O.; Albeck, S.; Houk, K. N.; Tawfik, D. S.; Baker, D. *Nature* **2008**, *453*, 190–195.
(6) Rosenblatt, M. M.; Wang, J.; Suslick, K. S. *Proc. Natl. Acad. Sci. U.S.A.* **2003**, *100*, 13140–13145.
(7) Ghirlanda, G. *Curr. Opin. Chem. Biol.* **2009**, *13*, 643–651.
(8) Reedy, C. J.; Gibney, B. R. *Chem. Rev.* **2004**, *104*, 617–650.
(9) Koder, R. L.; Anderson, J. L. R.; Solomon, L. A.; Reddy, K. S.; Moser, C. C.; Dutton, P. L. *Nature* **2009**, *458*, 305–309.
(10) Bender, G. M.; Lehmann, A.; Zou, H.; Cheng, H.; Fry, H. C.; Engel, D.; Therien, M. J.; Blasie, J. K.; Roder, H.; Saven, J. G.; DeGrado, W. F. *J. Am. Chem. Soc.* **2007**, *129*, 10732–10740.
(11) Jiang, L.; Althoff, E. A.; Clemente, F. R.; Doyle, L.; Röthlisberger, D.; Zanghellini, A.; Gallaher, J. L.; Betker, J. L.; Tanaka, F.; Barbas, C. F.; Hilvert, D.; Houk, K. N.; Stoddard, B. L.; Baker, D. *Science* **2008**, *319*, 1387–1391.
(12) Ye, S.; Discher, B. M.; Strzalka, J.; Noy, D.; Zheng, S.; Dutton, P. L.; Blasie, J. K. *Langmuir* **2004**, *20*, 5897–5904.
(13) Noy, D.; Discher, B. M.; Rubtsov, I. V.; Hochstrasser, R. M.; Dutton, P. L. *Biochemistry* **2005**, *44*, 12344–12354.
(14) Discher, B. M.; Noy, D.; Strzalka, J.; Ye, S.; Moser, C. C.; Lear, J. D.; Blasie, J. K.; Dutton, P. L. *Biochemistry* **2005**, *44*, 12329–12343.
(15) Ye, S.; Discher, B. M.; Strzalka, J.; Xu, T.; Wu, S. P.; Noy, D.; Kuzmenko, I.; Gog, T.; Therien, M. J.; Dutton, P. L.; Blasie, J. K. *Nano Lett.* **2005**, *5*, 1658–1667.
(16) Cordova, J. M.; Noack, P. L.; Hilcove, S. A.; Lear, J. D.; Ghirlanda, G. *J. Am. Chem. Soc.* **2007**, *129*, 512–518.
(17) McAllister, K. A.; Zou, H.; Cochran, F. V.; Bender, G. M.; Senes, A.; Fry, H. C.; Nanda, V.; Keenan, P. A.; Lear, J. D.; Saven, J. G.; Therien, M. J.; Blasie, J. K.; DeGrado, W. F. *J. Am. Chem. Soc.* **2008**, *130*, 11921–11927.
(18) Cochran, F. V.; Wu, S. P.; Wang, W.; Nanda, V.; Saven, J. G.; Therien, M. J.; DeGrado, W. F. *J. Am. Chem. Soc.* **2005**, *127*, 1346–1347.
(19) Walters, R. F. S.; DeGrado, W. F. *Proc. Natl. Acad. Sci. U.S.A.* **2006**, *103*, 13658–13663.
(20) Berry, E. A.; Walker, F. A. *J. Biol. Inorg. Chem.* **2008**, *13*, 481–498.
(21) Holmes, A. E.; Das, D.; Canary, J. W. *J. Am. Chem. Soc.* **2007**, *129*, 1506–1507.
(22) Walker, F. A. *Chem. Rev.* **2004**, *104*, 589–616.
(23) Yatsunyk, L. A.; Dawson, A.; Carducci, M. D.; Nichol, G. S.; Walker, F. A. *Inorg. Chem.* **2006**, *45*, 5417–5428.
(24) T'sai, A. L.; Palmer, G. *Biochim. Biophys. Acta* **1983**, *722*, 349–363.

JA107487B